SLAC-PUB-11135
April 2005
astro-ph/0504363

THE GROWTH, POLARIZATION, AND MOTION OF THE RADIO AFTERGLOW FROM THE GIANT FLARE FROM SGR 1806-20

G. B. TAYLOR [1,2], J.D. GELFAND [3], B.M. GAENSLER [3], J. GRANOT [1], C. KOUVELIOTOU [4], R. P. FENDER [5], E. RAMIREZ-RUIZ [6], D. EICHLER [7], Y. E. LYUBARSKY [7], M. GARRETT [8], & R. A. M. J. WIJERS [9]

Draft version April 16, 2005

ABSTRACT

The extraordinary giant flare (GF) of 2004 December 27 from the soft gamma repeater (SGR) 1806-20 was followed by a bright radio afterglow. We present an analysis of VLA observations of this radio afterglow from SGR 1806-20, consisting of previously reported 8.5 GHz data covering days 7 to 20 after the GF, plus new observations at 8.5 and 22 GHz from day 24 to 81. For a symmetric outflow, we find a deceleration in the expansion, from $\sim$4.5 mas/day to $<$2.5 mas/day. The time of deceleration is roughly coincident with the rebrightening in the radio light curve, as expected to result when the ejecta from the GF sweeps up enough of the external medium, and transitions from a coasting phase to the Sedov-Taylor regime. The radio afterglow is elongated and maintains a 2:1 axis ratio with an average position angle of -40° (north through east), oriented perpendicular to the average intrinsic linear polarization angle. We also report on the discovery of motion in the flux centroid of the afterglow, at an average velocity of 0.26 ± 0.03 c (assuming a distance of 15 kpc) at a position angle of -45°. This motion, in combination with the growth and polarization measurements, suggests an initially asymmetric outflow, mainly from one side of the magnetar.

Subject headings: pulsars: individual (SGR 1806-20) – stars: neutron – stars:flare – stars: winds,outflows – radio continuum: general

1. INTRODUCTION

The spectacular giant flare (GF) of 2004 Dec. 27 from the soft gamma repeater (SGR) 1806-20 is believed to have originated from a violent magnetic reconnection event in this magnetar (Palmer et al. 2005; Hurley et al. 2005). This sudden energy release of more than 10^{46} ergs in gamma-rays (assuming isotropic emission at a distance of 15 kpc) managed to eject a significant amount of baryons, probably accompanied by some pairs and magnetic fields, from the neutron star (Palmer et al. 2005; Gelfand et al. 2005; Granot et al. 2005). As this outflow interacted with the external medium, it powered an expanding radio afterglow (Cameron & Kulkarni 2005; Gaensler et al. 2005) at least 500 times more luminous than the only other radio afterglow detected from an SGR GF (Frail, Kulkarni & Bloom 1999). After an initially steep decay ($\sim t^{-2.7}$; Gaensler et al. 2005), a rebrightening in the radio light curve was seen, starting at $t \sim 25$ days and peaking at $t \sim 33$ days (Gelfand et al. 2005), followed by a shallower decay. This is most naturally explained by the transition from free expansion to the Sedov-Taylor phase, which occurs when a sufficient mass of ambient medium is swept up (Gelfand et al. 2005; Granot et al. 2005).

In this *Letter* we report on 8.5 GHz and 22 GHz radio observations with the Very Large Array (VLA) of the NRAO[10] between 7 and 81 days after the GF. These observations are used to measure the size, shape, motion and polarization properties of the radio afterglow. Assuming that SGR 1806-20 is at a distance of $15 d_{15}$ kpc (Corbel & Eikenberry 2004; McClure-Griffiths & Gaensler 2005), it is useful to remember that 1 mas corresponds to $15 d_{15}$ AU or $2.25 \times 10^{14} d_{15}$ cm. The radio observations are described in §2. In §3 we perform fits for the shape and size of the radio image using the visibility data. Our results are presented in §4 and discussed in §5.

2. OBSERVATIONS

VLA observations of SGR 1806-20 began 6.9 days after the GF with the VLA in its A configuration. Here we report all 8.5 GHz and 22 GHz observations up through day 81 (see Table 1). The first 20 days of monitoring with a host of radio telescopes including the VLA have previously been described by Gaensler et al. (2005) and by Cameron et al. (2005). Absolute flux calibration was obtained from a short observation of 3C286 during each run. Phase calibration was determined by observations of the strong (0.75 Jy) but somewhat distant (5.78 deg) calibrator PMN J1820-2528, or (from 2005 Jan. 16 on) the nearby (0.77 deg), and moderately strong (0.32 Jy) calibrator TXS J1811-2055 with a cycle time of 3.5 minutes. From Jan. 16 onwards, the validity of the phase transfer at 8.5 GHz was checked by short observations of J1820-2528 every 15 minutes. In general the coherence was found to be better than 95% on J1820-2528. For all observations except 2005 Jan. 3 the strong and unpolarized source, OQ208, was observed for 1 minute in order to permit solving for the instrumental polarization. For the data on Jan. 3, leakage terms were transfered from observations of BL Lac on 2005 Jan. 2. The absolute polarization angle was referenced to 3C286 for all epochs.

[1] Kavli Institute of Particle Astrophysics and Cosmology, Menlo Park, CA 94025, USA
[2] National Radio Astronomy Observatory, Socorro, NM 87801, USA
[3] Harvard-Smithsonian Center for Astrophysics, 60 Garden Streen, Cambridge, MA 02138, USA
[4] NASA/MSFC, XD-12, NSSTC, 320 Sparkman Dr., Huntsville, AL 35805, USA
[5] School of Physics and Astronomy, University of Southampton, Highfield, Southampton SO17 1BJ, UK
[6] IAS, Einstein Drive, Princeton, NJ 08540, USA
[7] Dept. of Phys., BGU, P.O. Box 653, Beér Sheva 84105, Israel
[8] Joint Institute for VLBI in Europe, Postbus 2, 7990 AA, Dwingeloo, The Netherlands
[9] Astronomical Institute "Anton Pannekoek", University of Amsterdam, Kruislaan 403, 1098 SJ, Amsterdam, The Netherlands

[10] The National Radio Astronomy Observatory is operated by Associated Universities, Inc., under cooperative agreement with the National Science Foundation.

Submitted to Astrophys.J.Lett.
Work supported in part by the Department of Energy contract DE-AC02-76SF00515

3. MODEL FITTING AND ERROR ANALYSIS

In all observations reported here the radio afterglow of SGR 1806-20 is smaller than the naturally weighted synthesised beam. Since the signal to noise is high, however, it is quite feasible to extract information about the size and shape of the source by fitting models to the visibility data. For each of the epochs we fit a two component model to the data for the SGR 1806-20 field. One elliptical, two-dimensional Gaussian component (with the 6 free parameters given in Table 2) describes SGR 1806-20 while a point source (not listed) was used to describe the radio nebula associated with the LBV star approximately 14 arcseconds to the East (Frail et al. 1997). Other models for the radio afterglow, including an elliptical ring, a uniform sphere, an elliptical disk, and two point sources, were tried but not found to provide a better fit. Fitting the VLA data to an elliptical ring, or disk at any epoch increases the derived size by a factor ∼1.16 and ∼1.66 respectively as expected (Pearson 1999). The model fitting was performed in both MIRIAD (task UVFIT) and Difmap and found to agree to within the uncertainties. We adopt the MIRIAD fits (Table 2) and the estimated statistical errors. As in Taylor et al. (2004) the error of the size was checked with Monte-Carlo simulations of the data using identical (u,v) coverage, similar noise properties, and a Gaussian component of known size added. The simulations confirm the error estimates quoted by MIRIAD, and agree with errors estimated from the signal to noise ratio and the synthesised beam shape.

In the early epochs there is some evidence from the MERLIN and VLBA observations (Fender et al. 2005) that the morphology of the source is more complicated than an elliptical Gaussian, and may experience rapid changes in the location of the peak emission. These changes in the suface brightness could cause shifts in the centroid of our model fits, and deviations in the fitted size. For this reason we have added a 10% error in quadrature to the measured size of all points, though the error may be larger in the earlier measurements. At later times the MERLIN observations seem to be more consistent with a smooth elliptical Gaussian, though it is worth noting that this observation was also at a lower frequency.

4. RESULTS

4.1. *Polarization*

Linear polarization from the radio afterglow was detected during the first 20 days after the GF at 8.5 GHz (Gaensler et al. 2005). Thereafter we were only able to measure upper limits on the polarization (Fig. 1). The polarization is found to be 2.1% on day 7 and to decrease to a minimum of 1.1% on day 10. At that time the linear polarization began to increase steadily to a maximum value of 3.4 % while the polarization angle swung rapidly from 4° to 40°. The polarization falls below our detection limit of 2% around the time of the rebrightening in the light curve. Limits as late as 55 days after the GF are below 2%.

4.2. *Expansion*

In Fig. 2 we plot the geometric mean radius of the elliptical Gaussian model fits. These fits show the expansion of the radio afterglow from SGR 1806-20 over the first 81 days after the GF. As reported in Gaensler et al. (2005) SGR 1806-20 was clearly resolved in the earliest VLA observations taken 7 days after the GF with a radius of ∼29 mas (mean half-width). MERLIN observations (Fender et al. 2005) reveal that the source is asymmetric, with a compact component and a long, broad extension. The size and position angle of the MERLIN extension at −31 degrees is roughly consistent with our average value of −40 ± 20. There is some possible evidence for a gradual swing in the position angle of the VLA data (Table 2), and we will investigate its significance in a future paper. Assuming a symmetric expansion, the velocity required to reach 29 mas in 7 days is 4.1 ± 0.6 mas/day (0.36 ± 0.05 $d_{15}c$). The estimated reflection symmetric expansion is $0.25 d_{15}c$ along the minor axis and $0.5 d_{15}c$ along the major axis.

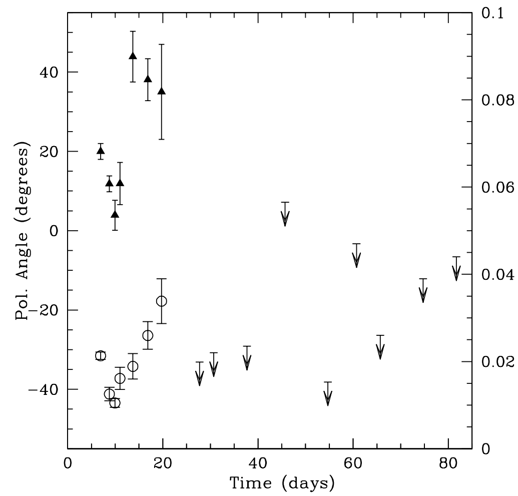

FIG. 1.— Linear fractional polarization (circles; right y-axis) and polarization angles (triangles; left y-axis) for the radio afterglow from SGR 1806-20 as a function of time at 8.5 GHz. All polarization angles have been corrected for the observed RM of 272 ± 10 rad m^{-2} (Gaensler et al. 2005). Limits on fractional polarization are drawn at 3σ.

After 30 days (the time of the rebrightening reported by Gelfand et al. 2005) the radio afterglow had grown to ∼ 133 mas (half-width). Between 7 and 30 days the expansion velocity continues to be high with an average velocity of 4.5 ± 0.8 mas/day (0.39 ± 0.07 $d_{15}c$). After this time, the growth appears to slow so that the average velocity between day 30 and the last day of observations reported here is 0.5 ± 1 mas/day ($< 0.2 d_{15}c$) where the source size reaches ∼161 mas. This expansion is in agreement with the MERLIN size estimate of ∼110 mas, 56 days after the GF.

Following Gelfand et al. (2005) (see their Eq. 4), we fit to the data from day 9 onwards a supersonically expanding shell that is decelerated as it sweeps up material. This fit (reduced χ^2 of 0.76; shown as the solid line in Fig. 2) implies a deceleration time of 40 ± 13 days after the GF, consistent with the time of the peak rebrightening at day ∼30 and the deceleration time of ∼46 days derived from the rebrightening (Gelfand et al. 2005). We also fit a constant expansion (2.8 ± 0.3 mas/day) to the data and obtain a reduced χ^2 of 1.22. An F-test gives a probability of 2% that the constant expansion is an equally valid description of the data. A broken power-law actually fits much better than either model (reduced χ^2 = 0.06), but requires both acceleration and deceleration of the explosion. The low χ^2 value of the broken power-law may indicate that we have been too conservative with our error estimation.

4.3. *Proper Motion*

Good astrometry was obtained for the radio afterglow from SGR 1806-20 on all days of the observations except 2005 Jan. 3, Jan. 10, and Feb. 7 via phase referencing to a nearby cal-

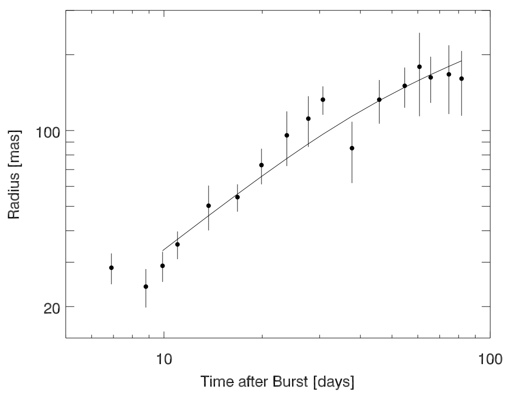

FIG. 2.— Expansion of the radio afterglow from SGR 1806-20 as a function of time. The size shown is the geometric mean of the semi-major and semi-minor axes of the best fitting elliptical Gaussian for each observation. The solid line is a fit of a supersonically expanding shell model as described by Eq. 4 of Gelfand et al. (2005).

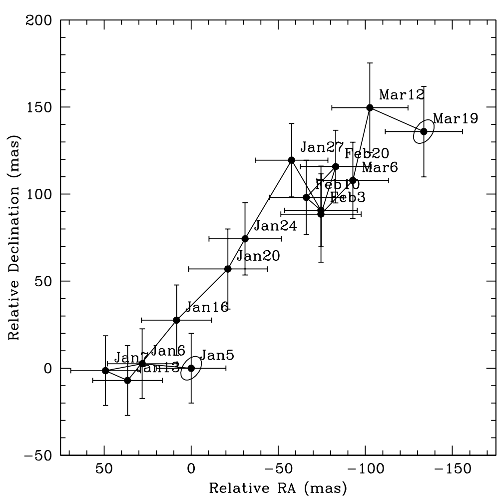

FIG. 3.— The trajectory of the afterglow of SGR 1806-20. Dates are labeled. The small ellipses denote the first and last days used.

ibrator. A combination of a long cycle time (15 min), distant calibrator (J1820-2528), and poor atmospheric phase stability resulted in a large systematic position error on Jan. 3, though changes in the relative brightness of different parts of the image (Fender et al. 2005) may also have affected the centroid position. On Jan. 10 the low elevation of the observations forced us to employ a distant calibrator with a poor position. On Feb. 7 poor weather caused unstable phase conditions such that the coherence estimated on J1820-2528 was only 36%.

The centroid of the radio afterglow from SGR 1806-20 is found to shift by $\sim$200 mas over the course of 70 days of observations (Fig. 3). We have decomposed the position into x and y components and show the least square fits to the position with time in Fig. 4. The radial proper motion is 3.0 ± 0.34 mas/day at a position angle of $-44 \pm 6\,^{\circ}$ (measured north through east). This motion corresponds to $0.26 \pm 0.03 d_{15} c$. There is some indication that the time of fastest proper motion also corresponds to the time of fastest growth.

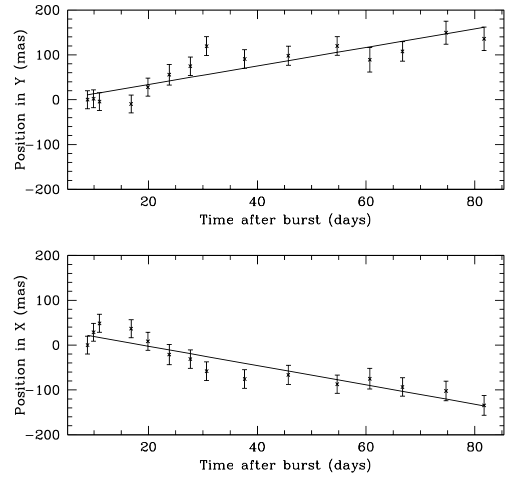

FIG. 4.— Proper motion of the afterglow of SGR 1806-20. The motion has been decomposed into Right Ascension and Declination components of motion.

5. DISCUSSION

The motion of the radio flux centroid is along the major axis of the source and is roughly half of the growth rate. This may be naturally explained by a predominantly one-sided outflow, which produces a radio nebula extending from around the location of the magnetar out a particular preferred direction corresponding to the direction of the ejection. This suggests that either the catastrophic reconfiguration of the magnetic field which caused the GF was relatively localized, rather than a global event involving the whole magnetar (c.f., Eichler 2002), or that the baryonic content of the ejecta is highly asymmetric.

The position angle of the linear polarization is roughly perpendicular to the major axis of the image and to the direction of motion of the flux centroid. This naturally arises for a shock-produced magnetic field, which is tangled predominantly within the plane of the shock (Medvedev & Loeb 1999), because of the elongated shape of the emitting region and due to projection effects (Gaensler et al. 2005). Alternatively, this might be caused by shearing motion along the sides of the one-sided outflow, which can stretch the magnetic field in the emitting region along its direction of motion.

The polarization is detected up to 20 days. During this time the emission is attributed to the shocked ejecta and a shocked external shell (Gaensler et al. 2005; Gelfand et al. 2005; Granot et al. 2005). If the emission is mostly from the shocked ejecta, then the degree of polarization of a few percent suggests that the magnetic field in the ejecta is not dominated by a magnetic field component ordered on large scales, but is instead tangled on relatively small scales. A similar conclusion is reached for GRB outflows, from 'radio flare' observations (Granot & Taylor 2005). If, on the other hand, the emission is dominated by the shocked external shell (as suggested by the dynamics; Granot et al. 2005) then the degree of polarization of a few percent might suggest that the doubly shocked material in the external shell has a magnetic field that is not predominantly ordered on large scales.

The degree of polarization decreased at about the same time as the deceleration and rebrightening in the light curve (see Fig. 1). As the rebrightening is attributed to the emission from the shocked external medium becoming dominant (Gelfand et al. 2005; Granot et al. 2005), this suggests a lower

TABLE 1
OBSERVATIONAL SUMMARY

Date	t (days)	Freq. (GHz)	Phase Calibrator	Time (min)	RMS noise (μJy/beam)	Array Config.	$B_{\rm min}$ (mas)	$B_{\rm maj}$ (mas)	$B_{\rm P.A.}$ (deg.)
2005 Jan 3	6.9	8.5	J1820-2528	12	60	A	222	458	16
2005 Jan 5	8.8	8.5	J1820-2528	15	70	A	213	542	–27
2005 Jan 6	9.9	8.5	J1820-2528	34	34	A	233	430	19
2005 Jan 7	11.0	8.5	J1820-2528	18	61	A	233	717	41
2005 Jan 10	13.7	8.5	J1751-2524	26	45	A	228	811	–41
2005 Jan 13	16.8	8.5	J1820-2528	38	25	A	295	597	29
2005 Jan 16	19.9	8.5	J1811-2055	28	31	A	408	605	–42
2005 Jan 20	23.8	22.5	J1811-2055	37	59	BnA	190	317	–75
2005 Jan 24	27.7	8.5	J1811-2055	21	30	BnA	451	1004	–60
2005 Jan 27	30.7	8.5	J1811-2055	32	36	BnA	382	1346	53
2005 Feb 3	37.7	8.5	J1811-2055	21	40	BnA	437	1062	–60
2005 Feb 7	41.7	8.5	J1811-2055	21	–	BnA	–	–	–
2005 Feb 11	45.7	8.5	J1811-2055	17	40	BnA	401	1328	–55
2005 Feb 20	54.7	8.5	J1811-2055	111	15	B	736	1323	–14
2005 Feb 26	60.7	8.5	J1811-2055	17	48	B	706	1465	–22
2005 Mar 4	66.7	8.5	J1811-2055	66	36	B	720	1296	3
2005 Mar 12	74.7	8.5	J1811-2055	26	42	B	730	1305	3
2005 Mar 19	81.7	8.5	J1811-2055	37	44	B	736	1351	14

*NOTE - VLA data from Feb. 7 was unusable due to poor observing conditions. Feb. 11 includes data taken on Feb 10 and Feb 12. Feb. 20 includes data taken on Feb. 19 and Feb. 21. Column 2 gives t, the time after the GF, column 5 refers to the total integration time on source, and $B_{\rm maj}$, $B_{\rm min}$, and $B_{\rm P.A.}$ describe the naturally weighted synthesized restoring beam measured north through east.

polarization of this emission component. This, in turn, suggests that the magnetic field in the shocked ISM is less ordered than in the shocked ejecta and/or shocked external shell. Such a difference might occur if the magnetic field in the shocked ISM is predominantly shock-produced, while that in the shocked ejecta can have a significant ordered component advected from the source. Moreover, the shocked external shell, even if predominantly shock-produced, might still be more ordered due to the additional compression of the shell.

The leading edge of the radio afterglow from the GF is moving at the sum of the apparent proper motion and expansion velocities. As this may approach c at early times, this could dominate the energetics of the outflow. This effect is not included in the simple expansion model we have fit to the data, and should be investigated further.

6. CONCLUSIONS

We report a deceleration in the observed expansion of the radio afterglow produced by the 2004 Dec. 27 Giant Flare from SGR 1806-20. We also find a proper motion for the radio afterglow roughly aligned with its major axis and perpendicular to the average polarization angle. These observations support the idea of an asymmetric explosion on one side of the magnetar. The polarization data place significant constraints on the magnetic field structure in the shocked ejecta and ISM. Measurements with the VLA continue, and will be presented in a future paper.

J.D.G. and B.M.G. acknowledge the support of NASA through LTSA grant NAG5-13032. J.G. acknowledges support from the US Department of Energy under contract number DE-AC03-76SF00515. D.E. acknowledges support from the Israel-U.S. BSF, the ISF, and the Arnow Chair of Physics. Y.L acknowledges support from the German-Israeli Foundation. E.R.R is sponsored by NASA through a Chandra Postdoctoral Fellowship award PF3-40028. R.A.M.J.W acknowledges support from NWO.

REFERENCES

Cameron, P. B., & Kulkarni, S. R. 2005, GCN Circ., 2928
Cameron, P. B. et al. 2005, submitted, astro-ph/0502428
Corbel, S., & Eikenberry, S. S. 2004, A&A, 419, 191
Eichler, D. 2002, MNRAS, 335, 883
Fender, R. P., et al. 2005, in preparation
Gaensler, B. M., et al. 2005, Nature, in press, astro-ph/0502393
Gelfand, J. D., et al. 2005, submitted to ApJL (astro-ph/0503269)
Frail, D. A., Vasisht, G., & Kulkarni, S. R. 1997, ApJ, 480, L129
Frail, D. A., Kulkarni, S. R., & Bloom, J. S. 1999, Nature, 398, 127
Granot, J., et al. 2005, submitted to ApJL (astro-ph/0503251)
Granot, J., & Taylor, G. B. 2005, ApJ, in press (astro-ph/04120309)
Hurley, K. et al. 2005, Nature, in press, astro-ph/0502329
McClure-Griffiths, N.M., & Gaensler, B.M. 2005, astro-ph/0503171
Medvedev, M. V., & Loeb, A. 1999, ApJ, 526, 697
Palmer, D. M. et al. 2005, Nature, in press, astro-ph/0503030
Pearson, T. J. 1999, ASP Conf. Ser. 180: Synthesis Imaging in Radio Astronomy II, 180, 335
Taylor, G. B., Frail, D. A., Berger, E., and Kulkarni, S. R. 2004, ApJ, 609, L1

TABLE 2
MODEL FITTING AND POLARIMETRY RESULTS

t (days)	Flux (mJy)	Δ x (mas)	Δ y (mas)	θ_M (mas)	Axial Ratio	θ_{PA} (deg.)	Pol. (%)	ϕ (deg.)
6.9	54.59±0.09	–	–	79.4±0.9	0.52±0.06	–58±2	2.1 ± 0.1	20 ± 2
8.8	32.30±0.09	0	0	67.8±4.9	0.50±0.12	–65±8	1.3 ± 0.2	12 ± 2
9.9	23.68±0.04	28	2	78.6±1.2	0.55±0.06	–52±3	1.1 ± 0.1	4 ± 4
11.0	16.78±0.06	47	–5	85.8±2.4	0.68±0.03	–68±12	1.6 ± 0.3	12 ± 5
13.7	9.75±0.05	–	–	120.3±16.3	0.70±0.10	–59±12	1.9 ± 0.3	44 ± 6
16.8	5.65±0.04	37	–9	121.6±5.9	0.80±0.13	–87±24	2.6 ± 0.3	38 ± 5
19.9	4.18±0.05	10	26	197.7±12.8	0.54±0.08	–54±8	3.4 ± 0.5	35 ± 12
23.8	1.62±0.12	–19	56	208.9±40.7	0.84±0.25	–31±46	–	–
27.7	3.24±0.06	–36	71	276.1±42.3	0.65±0.12	–44±11	<2.0	
30.7	3.93±0.06	–68	111	292.3±17.7	0.82±0.22	–26±31	<2.2	
37.7	3.22±0.06	–70	91	258.3±37.5	0.43±0.26	–15±16	<2.4	
45.7	2.60±0.05	–61	97	346.4±38.9	0.59±0.11	–26±10	<5.7	
54.7	2.03±0.03	–78	109	352.5±41.7	0.73±0.10	–21±11	<1.5	
60.7	1.78±0.07	–67	75	461.4±117	0.60±0.30	–28±17	<4.7	
65.7	1.72±0.04	–92	107	446.8±50.6	0.53±0.09	–12±7	<2.6	
74.7	1.55±0.06	–113	128	446.1±90.3	0.56±0.16	–11±13	<3.9	
81.7	1.39±0.05	–135	141	459.1±78.6	0.49±0.22	–23±15	<4.4	

*NOTE - Positions are relative to that derived on Jan. 5 which is RA 18 08 39.3418, DEC –20 24 39.827 (J2000). The positions of Jan. 3 and 10 are excluded for reasons described in the text. The errors quoted on the flux densities are only statistical, and will be discussed in a future paper. Position errors are dominated by a ~20 mas systematic uncertainty in the astrometry. The source size is described by the major axis, θ_M, axial ratio, and position angle $\theta_{P.A.}$. Note that the PA at 13.7 days after the burst differs substantially from the value of 62 ± 14 deg shown in Fig 3 of Gaensler et al (2005). The new fit presented here seems more consistent with the PA's seen at adjacent epochs. A subsequent paper will fully investigate this possible discrepancy. The source polarization is described by the fractional polarization in % and the electric vector polarization angle, ϕ, where ϕ has been corrected for the observed RM of 272 ± 10 rad m^{-2} (Gaensler et al. 2005)